Journal of Hazardous Materials, 22 (1989) 331-357
Elsevier Science Publishers B.V., Amsterdam — Printed in The Netherlands

ATMOSPHERIC DISPERSION OF TOXIC GASES IN A COMPLEX ENVIRONMENT

E. VERGISON, J. VAN DIEST and J.C. BASLER

Solvay & Cie, S.A., rue de Ransbeek 310, 1120 Brussels (Belgium)

(Received May 10, 1988; accepted in revised form June 6, 1989)

Summary

This paper describes a study which was initiated by the BITC (Bureau International Technique du Chlore) and carried out at the Von Karman Institute for Fluids Dynamics and the Solvay Research Laboratory in Brussels.

The main purpose of the project was the setting up of a suitable mathematical model and associated computer code to describe the down-wind dispersion of gaseous releases in real sites including industrial environments. Both theoretical and experimental studies were performed and have led to a model describing the behaviour of toxic gases in a medium sized domain.

In studies on toxic gases, typical concentrations are usually low and the "hazard range" we are interested in is a long way from the source. Source effects, in this context, are considered to have such a limited influence that they can be neglected.

The model can deal with a wide variety of sources (jets, stacks, area sources) and releases (instantaneous, short duration continuous). Moreover, obstacles can be interposed upwind and/or downwind of the release point and real topography can be satisfactorily modelled.

The model has been extensively validated against wind tunnel experiments and against other models used in atmospheric dispersion prediction. Close agreement has also been found between BITC model predictions and data obtained at full scale during the China Lake experiments. The BITC model is also able to show the influence of the pollutant density and the enhancement of dispersion in the presence of obstacles.

On the basis of the validation tests carried out and the consistent results obtained, it is concluded that the BITC model can be regarded as a robust and reliable tool for predicting gas dispersion. Moreover, the BITC model program code has been written so that it can be run on medium-sized computers.

We consider that the dispersion model here described is not just another one in an already too long list but that it constitutes a definite improvement in assessing the effect of obstacles on the dispersion.

1. Introduction

Since 1980, the BITC, which is an association of European chlorine manufacturers, has been deeply involved in theoretical and experimental studies concerning the atmospheric dispersion of heavy gases in complex environments.

A theoretical study conducted at the Von Karman Institute (VKI) by Fous-

0304-3894/89/$03.50

sat in the early eighties [1,2] had led to a mathematical model describing near-field turbulent dispersion of gases of any density in complex environments. Different atmospheric types were also taken into account.

Subsequently, VKI, the Catholic University of Leuven and Solvay worked together to make significant improvements in the K-model, so that the current version consists of a computer code that calculates unsteady concentrations profiles in a previously calculated, steady turbulent velocity field [3].

The mathematical model has been designed to meet the following challenging objectives:

- it should be applicable to the study of toxics (rather than flammable gases) characterized by low concentrations at distances a long way from the source,
- it should be sufficiently rigourous to handle atmospheric turbulence in complex domains over a full range of atmospheric conditions,
- it should be capable of dealing with both continuous and instantaneous releases of passive gases and also gases which may be lighter or heavier than air,
- it should be capable to be run on a departmental computer.

In the first part of this paper, we will review the basic physics incorporated in the model and develop it in mathematical form.

The second part is devoted to the methodology that was developed in order to validate the model against wind tunnel and field test experiments on the one hand, and to simulate practical industrial cases on the other.

We then discuss in detail the way in which the computer code has to be preprocessed in order to derive the relevant physical input values and how the test set was selected.

Finally, we will present some results obtained so far.

2. Theoretical approach and mathematical modelling

Insofar as Prandtl's concept of a purely laminar sub-layer near a smooth surface is not applicable to atmospheric flows, we have to introduce turbulence mechanisms in the conservation laws of fluid mechanics that express the problem mathematically.

The Reynolds decomposition [1,4] acting on the state variables — wind velocities, viscosities, pressures, temperatures and concentrations — allows us to separate the average value effect from its purely turbulent counterpart.

However, a full quantitative treatment of the derived system of equations would require a huge amount of both theoretical and computer work.

Nonetheless, we feel that it is possible, by a judicious choice of approximations, to keep the problem sufficiently rigourous and tractable for solving a large range of industrial scenarios [5].

The strategy that was followed, when starting to build a mathematical model for heavy gases, was first to make it work correctly for passive gases, which

means that intensive tests were carried out to validate the model against wind tunnel experiments [2,5,6], other models [3,5] (amongst which the Gaussian ones), and available literature [7,8].

In this early stage, a great deal of effort was invested in studying the overall characteristics of dispersion and the behaviour of a cloud in obstacle wakes, the presence of obstacles being for us a point of major concern [2,5].

Particular attention was also paid to result sensitivity on mathematical parametrization [1,5,9] (the mesh size in numerical discretization, the mathematical relaxation in the iterative solvers, the quantity of particles needed to simulate a gas cloud).

Assumption 1 — Incompressibility of the atmospheric flow

The atmospheric flow is assumed to be incompressible, which means that dynamic effects on compressibility can be neglected [4,5].

This neither means, however, that air flow is incompressible nor that thermodynamic changes with height will not generate significant changes in density.

In the latter case, temperature is assumed to be the main factor responsible for height–density variations.

Although we must be aware that, over a substantial range of applications, the source effects, where gravity spread dominates, interact with ambient turbulence effects, we have the feeling that, in the case of small up to medium size releases of toxic gases (no flammability problems), we are allowed to look at heavy gas releases as a transient disturbance of the atmospheric surface layer. The model describes the continuous transition from heavy gas controlled flow at ambient temperature to dispersion by ambient turbulent dispersion only.

Assumption 2 — Boussinesq approximation

Although atmospheric flow is considered to be incompressible, while density is essentially dependent on temperature, we will neglect density variations insofar as they affect inertia and retain them only when combined with the acceleration of gravity in the buoyancy term of the momentum equation [1,4,5].

Assumption 3 — Gradient transfer hypothesis for turbulence closure

The Reynolds decomposition [4], naturally induces turbulent stresses and heat fluxes which have to be modelled.

The closure adopted here is to assume that the turbulent stresses and heat fluxes are proportional to their mean value counterparts.

A major consequence of this type of closure is that the momentum and energy equations now contain viscous contributions which are important in the numerical method chosen for solving them.

Assumption 4 — Nee-Kovasnay turbulence model

By using the approach described, it is possible to model the turbulent stresses and heat fluxes that appear as a consequence of the Reynolds decomposition.

Essentially, this results in the introduction of a turbulent viscosity whose variation with height and downwind distance has not yet been made explicit.

The way this is dealt with in the model is due to Nee and Kovasnay [10], who treated both vertical and downwind turbulent viscosities as scalar quantities that are subject to classical conservation laws; that is as quantities which are transported by advection, which diffuse, which are produced and/or destroyed.

Moreover, they treated turbulent viscosity as a self-diffusive process, the diffusion coefficient being viscosity itself.

The original Nee–Kovasnay model has been extended [1,5] by adding a buoyancy production term in the vertical turbulent viscosity balance in order to reflect the effect of temperature stratification on turbulence.

Assumption 5 — The pollutant does not interact dynamically and thermically with air

It is assumed that any interaction between pollutant and air momentum can be neglected even in the source area [1,5].

This means that the pollutant does not influence significantly the momentum balance of the transporting fluid. It also means that whenever this assumption does not hold, in the case of high pressure jets for instance, we have to deal with the source term separately in order to estimate the gas cloud size at the end of this initial phase.

The two first stages following the release, i.e. the one where the turbulence generated by the accidental release process is important, and the second phase, in which the heavy gas cloud slumps as a gravity flow, are supposed to be studied separately in order to provide the necessary source characteristics to get the study started at a stage where the major effects are the cloud excess density and the ambient turbulence. Dilution effects for example, should be quantified separately. Assumption 5 is essential in the sense that it allows us to decouple the concentration diffusion equation from the turbulent flow balances.

The completed system of partial differential equations describing the turbulent flow field can now be written:

Mass

$$\frac{\delta s}{\delta x}+\frac{\delta w}{\delta z}=0, \tag{1}$$

Momentum

$$\frac{\delta u^2}{\delta x}+\frac{\delta(uw)}{\delta z}=\frac{\delta}{\delta x}\left(\mu_x\frac{\delta u}{\delta x}\right)+\frac{\delta}{\delta z}\left(3\mu_z\frac{\delta u}{\delta z}\right)-\frac{\delta\phi}{\delta x},$$

$$\frac{\delta(uw)}{\delta x}+\frac{\delta w^2}{\delta z}=\frac{\delta}{\delta x}\left(\mu_x\frac{\delta w}{\delta x}\right)+\frac{\delta}{\delta z}\left(\mu_z\frac{\delta w}{\delta z}\right)-\frac{\delta\phi}{\delta z}-g\frac{T-\theta_0}{\theta_0}, \tag{2}$$

Energy

$$\frac{\delta(uT)}{\delta x}+\frac{\delta(wT)}{\delta z}=\frac{\delta}{\delta x}\left(\mu_{T,x}\frac{\delta T}{\delta x}\right)+\frac{\delta}{\delta z}\left(\mu_{T,z}\frac{\delta T}{\delta z}\right), \tag{3}$$

Turbulence

$$\begin{aligned}\frac{\delta(u\mu_x)}{\delta x}+\frac{\delta(w\mu_x)}{\delta z}&=\frac{\delta}{\delta x}\left(\mu_x\frac{\delta\mu_x}{\delta x}\right)+\frac{\delta}{\delta z}\left(\mu_z\frac{\delta\mu_x}{\delta z}\right)\\&+A(\mu_x-\gamma)\left|\frac{\delta u}{\delta z}+\frac{\delta w}{\delta x}\right|-\frac{B}{L_d^2}\mu_x(\mu_x-\gamma),\\\frac{\delta(u\mu_z)}{\delta x}+\frac{\delta(w\mu_z)}{\delta z}&=\frac{\delta}{\delta x}\left(\mu_x\frac{\delta\mu_z}{\delta x}\right)+\frac{\delta}{\delta z}\left(\mu_z\frac{\delta\mu_z}{\delta z}\right)\\&+A(\mu_z-\gamma)\left|\frac{\delta u}{\delta z}+\frac{\delta w}{\delta x}\right|-\frac{B}{L_d^2}\mu_z(\mu_z-\gamma)+P_\theta.\end{aligned} \tag{4}$$

Here u denotes the mean horizontal wind velocity, w the mean vertical wind velocity, x downwind distance, z height, μ mechanical turbulent viscosity, ϕ kinematic pressure, g gravitational constant, T temperature, θ_0 reference potential temperature, γ kinematic air viscosity, A and B model constants, L_d^2 characteristic length scale, and P_θ is buoyancy production/loss term. All parameters are in SI units (see also Notation section). The buoyancy production/loss term P_θ is expressed using the gradient Richardson number (Ri_g) in the form:

$$P_\theta=-C\frac{Ri_g}{Pr_t}(\mu_z-\gamma)\left|\frac{\delta u}{\delta z}+\frac{\delta w}{\delta x}\right|,$$

where C is a model constant and Pr_t the turbulent Prandtl number. Adding natural boundary conditions:

- a given upstream velocity profile,
- ground level values for the state variables (null velocity, given temperature), as well as along buildings,
- continuous flux conditions elsewhere (downstream and along the upper boundary),

the system is then solved numerically by using an iterative procedure (time marching based on a marker and cell (MAC) finite difference scheme [11–13]).

The MAC method, which was originally developed for calculating transient flows, has been used in the present work, as an iterative technique for getting the steady state of the Navier–Stokes set of equations.

The original MAC technique was slightly adjusted by introducing an artificial viscous contribution [11], which places our formulation between the centered discretization and the full upstream one (Donor Cell).

Typically, we obtain for the convection terms, expressions like:

$$\frac{1}{4\delta y}[(v_{i,j}+v_{i+1,j})\ (u_{i,j}+u_{i,j+1})+\alpha|v_{i,j}+v_{i+1,j}|(u_{i,j}-u_{i,j+1})$$

$$-(v_{i,j-1}-v_{i+1,j-1})\ (u_{i,j-1}+u_{i,j})-\alpha|v_{i,j-1}+v_{i+1,j-1}|(u_{i,j-1}-u_{i,j})],$$

where α is an adjustable model parameter varying between 0 and 1; $\alpha=0$ leads to the original MAC formulation, while $\alpha=1$ corresponds to the Donor Cell one, which introduces a significant artificial viscosity. The latter, only influences the transient state and by no way, penalizes the steady state.

However, the damping introduced by this artificial viscosity, if not controlled, will strongly affect the computer code performances; that is why we choose α, slightly larger than the maximum value of the quantities

$$\left|\frac{u\delta t}{\delta x}\right| \quad \text{and} \quad \left|\frac{v\delta t}{\delta y}\right|$$

as close as possible to 1:

$$1\geqslant\alpha\geqslant\max\left\{\left|\frac{u\delta t}{\delta x}\right|,\left|\frac{v\delta t}{\delta y}\right|\right\}.$$

The restrictions made on the time step δt, mainly come from the fact that the finite difference forms of the continuous equations account for transfers between adjacent cells.

The condition:

$$\delta t\leqslant\min\left\{\frac{\delta x}{|u|},\frac{\delta z}{|w|}\right\}$$

which expresses the fact that the fluid is not allowed to flow across more than one computational cell in one time step, is natural in the sense that the convective flux approximations assume adjacent cell exchanges only.

On the other hand the "parabolic type" condition

$$\delta t\leqslant\frac{1}{2}\left[\frac{1}{(1/\delta x)^2+(1/\delta z)^2}\right]\min\ (1/\eta_x,1/\eta_z)$$

limits the speed at which momentum of heat diffuses, again in order to keep the phenomenon inside one cell.

It should be emphasized that this two-dimensional steady-state system of equations is solved independently from the pollutant dispersion balance, which is completely decoupled (Assumption 5) and simply expressed by the relation:

$$\frac{\delta c}{\delta t}+\frac{\delta}{\delta x}\left(c\left(u-\frac{\mu_x \delta c}{c\ \delta x}\right)\right)-\frac{\delta}{\delta y}\left(\mu_y \frac{\delta c}{\delta y}\right)+\frac{\delta}{\delta z}\left(c\left(w-\frac{\mu_z \delta c}{c\ \delta z}\right)\right)=S, \tag{5}$$

Notice that, in this three dimensional unsteady equation, the mass transfer coefficients are equal to the mechanical ones; this is due to the fact that their ratio — the Schmidt number — is assumed to be close to unity [5].

Equation (5) is solved by using a Lagrangian discretization technique, the pollutant being considered as the sum of a sufficiently large number of particles moving in the previously computed velocity field.

The diffusional velocities:

$$\frac{\mu_x}{c}\frac{\delta c}{\delta x} \quad \text{and} \quad \frac{\mu_z}{c}\frac{\delta c}{\delta z} \tag{6}$$

are replaced by randomized velocities [1,3]; the random displacement is assumed to be of Gaussian probability with standard deviation:

$$\sigma=\sqrt{2\mu_i \delta t}, \quad i=x, y, \tag{7}$$

δt being the time step. This formulation, however, seriously underestimates the mean plume rise in turbulent shear layers, in that the random displacement of a particle obeying a Gaussian law of zero mean and of variance given by eqn. (7) does not express the fact that turbulence influences the rise of the plume centroïd. A new approach, better suited for non-homogeneous turbulence was developed [6,14] by adding to the previous random displacement a term taking into account the tendency of the pollutant to be transported in the direction of increasing turbulent length scales. This term proportional to the gradients of the typical turbulent parameters, does account for the mean "turbulent" displacement of the plume centroïd.

3. Methodology for model validation

The model as described employs descriptive physical parameters which are likely to be unfamiliar to industrial users, who will tend to think in terms of stability classification schemes [15].

As a result, some additional work needs to be done to make the program better suited to practical applications.

Development work was carried out to the point where a fully integrated set of programs has been set up. These are easy to handle and make extensive use

of graphics both for testing mathematical convergence and picturing pollutant concentration profiles [3].

Finally, a broad range of test cases was developed, based on wind tunnel [1,16] and field test experiments [7,17,18] as well as on our own experience and current literature [14,15,19,20].

We will not dwell in this work on the important mathematical validation work that has been conducted by Foussat [1], Schreurs [5] and Vergison [9] in order to check the model mesh sizes, so as to find out the number of particles needed for simulating a cloud and, as well as to calibrate the overrelaxation parameters in the iterative MAC algorithm.

3.1 Physical data preprocessing

The mathematical model handles physical quantities such as the roughness height, the Monin–Obukhov length and the friction velocity, that are closely related both to the mechanically and thermally induced turbulence and to dispersive behavior of the atmospheric surface layer.

Industrial users will be more familiar with an expression of Pasquill stability classes, a typical velocity at reference height and roughness height as given in [21] and [22]. A precprocessor called METEO asks for these data in order to calculate the relevant information for running the code.

Some guidance is also provided in order to avoid inconsistent data as, for instance, incompatible stability classes and temperature gradients, wind speeds or insolation [21–23].

The physics upon which METEO is based essentially relates he Monin–Obukhov length [4,24], which expresses the height at which thermal stresses balance the mechanical ones, to practical data [3].

3.2 Fully integrated computer code

The computer code was built as a weakly coupled jigsaw, which means that each module (METEO preprocessor, turbulent flow field and dispersion calculations, graphical output and printouts) although precisely integrated in the whole procedure, as shown in Fig. 1 below, can be handled and controlled independently.

The sequence of operations starts with preprocessing the data, as just described. The turbulent flow field is then obtained as the asymptotic state of a time marching iterative procedure [1].

Convergence is established graphically by placing graphical "sensors" in the most turbulence sensitive parts of the domain (near buildings for instance). In this way we can check the convergence of all the state variables (velocities, viscosities, temperature and pressure) [3].

Establishing convergence this way avoids tedious manual examination of numerical printouts or non obvious, internally coded, automatic convergence

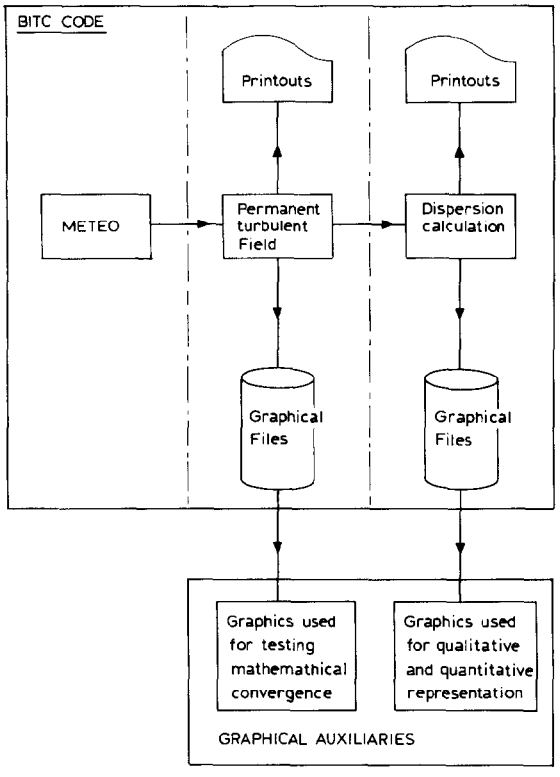

Fig. 1. Structure of the BITC code.

criteria. Intensive tests have been carried out to check the robustness of this approach.

Once the flow field converges for a given building configuration and fixed atmospheric class, we are then able to simulate a wide range of three dimensional dispersion scenarios, such as
puffs or continuous releases of any duration; various types, and sizes of sources (linear, surface or volume); gases which are passive, heavier of even lighter than air.

Cloud development can be followed either by analyzing the numerical output or again by using graphical tools. In the latter case, we can get both qualitative (pictures of the cloud) or quantitative (isoconcentrations lines) information.

A great deal of attention has also been given to ensuring that the computer code is portable: the language is ANSI-FORTRAN 77 and graphics are based on the Graphical Kernel System (G.K.S., an ISO norm). Minimal effort is required to implement the program on different machines.

3.3 Validation test sets

Validation of the BITC computer code was a key element of the study which was carried out both at the Von Karman Institute for Fluids Dynamics and at the Solvay Research Laboratory.

As mentioned previously, this validation required direct comparison with data obtained at full scale and from wind tunnel experiments. It was also necessary to check the BITC code against other computer codes currently used in atmospheric dispersion prediction.

A preliminary, but extensive, validation was undertaken at the Von Karman Institute for Fluid Dynamics by comparing calculated values with wind tunnel data.

Among these tests, $CBrF_3$ (molar mass 149 g) releases from an elevated point source ($z_{source}=0.05\delta$, where δ is the boundary layer thickness) in an artificially thickened turbulent boundary layer seem to be particularly significant [25]. The wind tunnel which had a 180 mm by 350 mm rectangular cross section was characterized by a 2 m long test section. Vortex generators and surface roughness were used to generate a turbulent mean velocity profile close to the one in the section atmospheric boundary layer.

Figure 2 compares the experimental and predicted decay of maximum concentration downstream of the source; apart from the near surroundings of the source, the two profiles are in agreement.

A more detailed study conducted by Riethmuller and Borrego [25] compares

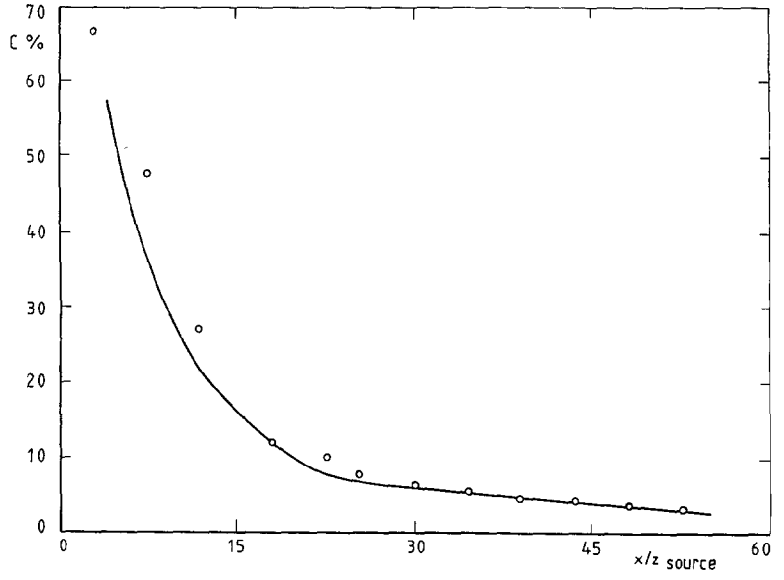

Fig. 2. Longitudinal decay of maximum concentration for heavy gas free dispersion from a point source. O Experiment, and — prediction.

predicted and experimental concentration profiles at different longitudinal locations (Fig. 3). Again the agreement is quite good apart from a slight underestimation of the plume spread quite near to the source; it leads us to emphasize that the present model represents a valid tool for the prediction of heavy gas dispersion in the atmospheric surface layer.

To ensure and check the robustness of the code and the validity of the basic physical hypotheses adopted, intensive tests were also carried out by Solvay to show:

- the consistency with Gaussian models in typical free-field situations,
- the effect of the pollutant density on the dispersion process,
- the influence of atmospheric stability,
- the effect of the wind speed on dispersion,
- the dependence on the pollutant release rate,
- the influence of the emission duration,

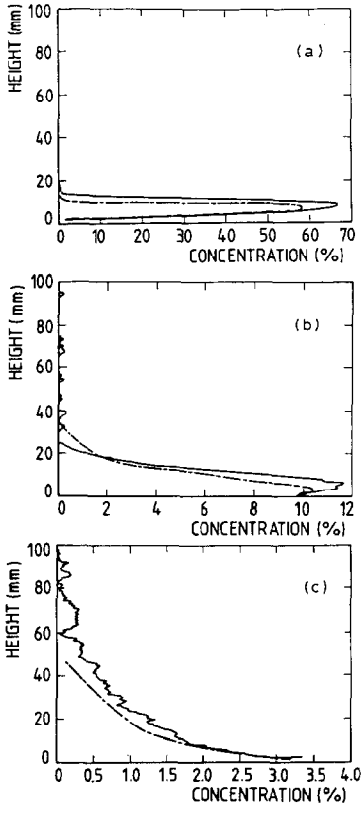

Fig. 3. Concentration profiles for heavy gas and point source in a simulated atmospheric boundary layer. $Vx=3x_{source}$ (a), $17x_{source}$ (b), and $50x_{source}$ (c) respectively. Prediction —·—, and — experiment.

- the prominent part played by buildings in the dispersion phenomena,
- good agreement with the results from the experimental releases of methane in the BURRO tests (China Lake Experiments) and from the Thorney Island tests.

More then 3000 hours CPU time were spent on a VAX 11/780. The results obtained and the conclusions which have been reached are summarized in the next section.

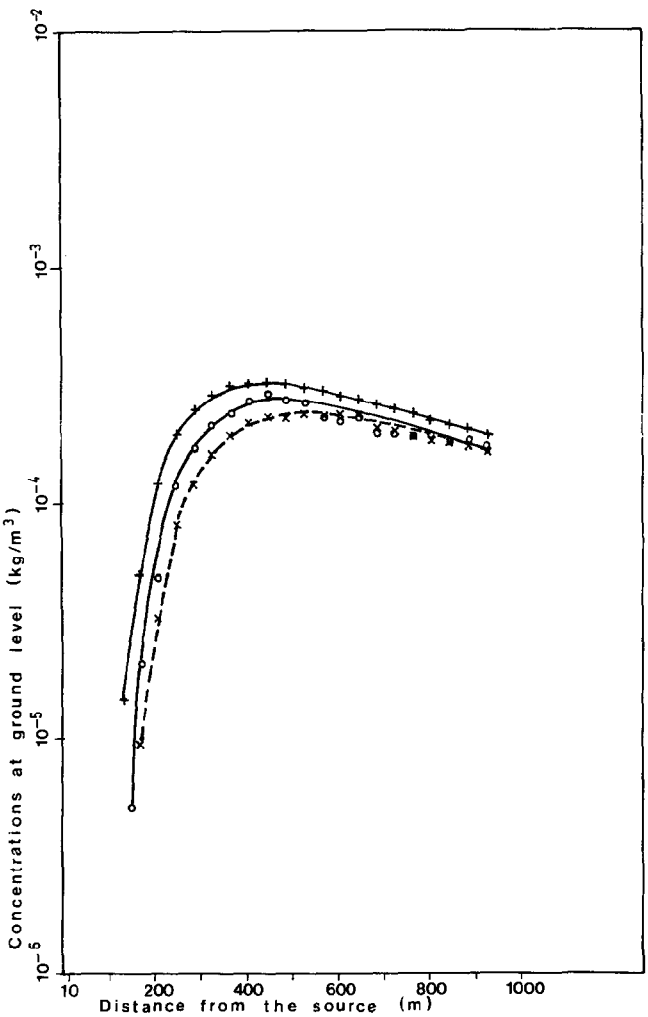

Fig. 4. Continuous emission from a chimney. Conditions: Neutral atmosphere D (free field), 30 m chimney, $Z_0 = 0.1$ m, $v_{10m} = 5$ m/s, $VT = -1\,°C/100$ m, and exhaust flowrate = 10 kg/s. Predictions by: + + Gaussian model, —O— BITC (heavy gas), and —×— BITC (passive gas).

4. Main results of the tests performed with the BITC computer code

4.1 Comparison with the Gaussian model in typical free field situations

The BITC program has been extensively checked against Gaussian predictions under different atmospheric stability categories (unstable, neutral and stable).

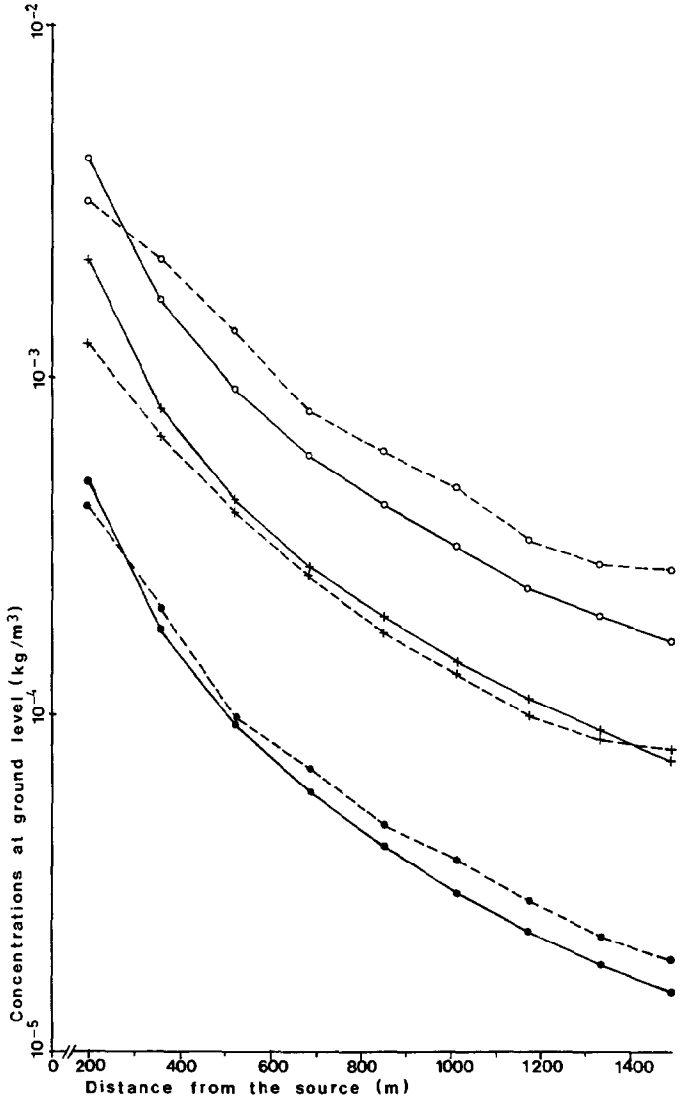

Fig. 5. Comparison between Gauss model and BITC model programs. Conditions: continuous emission, free field, passive gas, source at ground level, $Z_0 = 0.03$ m, $v_{10\,m} = 3$ m/s and flowrate = 1 kg/s. + + Neutral Gauss, −+− neutral BITC, −○− stable Gauss, − ○ − stable BITC, −●− unstable Gauss, and − ● − unstable BITC.

In the case of a passive gas emitted from a stack there was close agreement between BITC model predictions and Gaussian model predictions (see Fig. 4). This can be regarded as a worthwhile comparison, because under these conditions, the Gaussian model is usually regarded as reliable.

In the case of a passive gas emitted at ground level, there was good agreement between both models too (see Fig. 5) inspite of the fact that the Gaussian model is not really appropriate for emissions at ground level.

4.2 Influence of the pollutant density

Although the BITC model was initially aimed at predicting the dispersion of heavy gases, it can, in fact, predict the dispersion of a gas of any density provided we restrict ourselves to scenarios where the hazard range is sufficiently far from the source and the concentrations are low enough to avoid the source effects. Figure 4 shows the calculated effect of the pollutant density (a passive gas such as air, and chlorine have been used as examples).

In comparing the behaviour of passive and heavy gases, it is worth noting that the difference is very pronounced in the immediate and intermediate zones but rather small in the distant zone (beyond a few hundred meters from the source). This is due to the well known fact that the passive gas diffusion process represents the asymptotic far field behaviour of a heavy gas cloud.

In all the tests which were carried out, the plotting routines which were developed at the Solvay Computer Center proved particularly useful by pro-

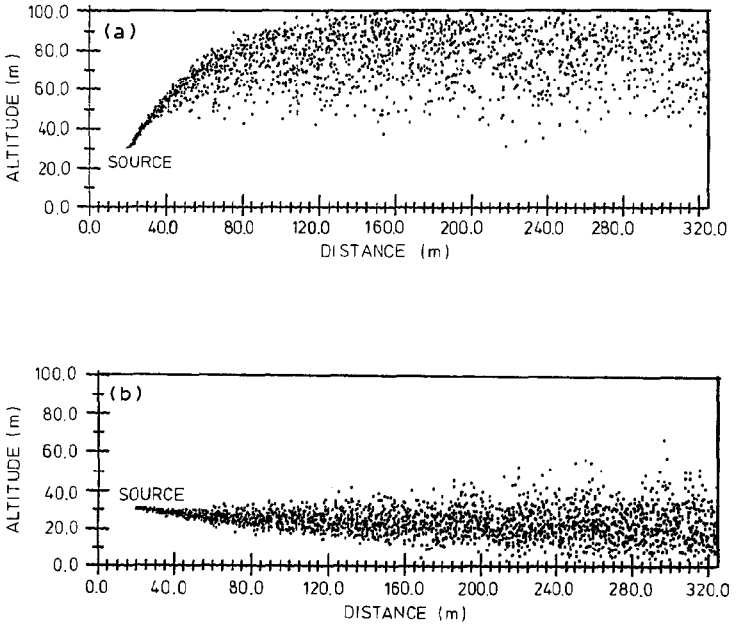

Fig. 6. Influence of the pollutant density of H_2 (a) and Cl_2 (b).

viding graphical outputs for the velocity field calculation and dispersion programs.

These plotting routines enable us to see the graphical distribution of the pollutant particles in the symmetry plane. Figure 6, for example, shows hydrogen and chlorine gas emissions from a stack.

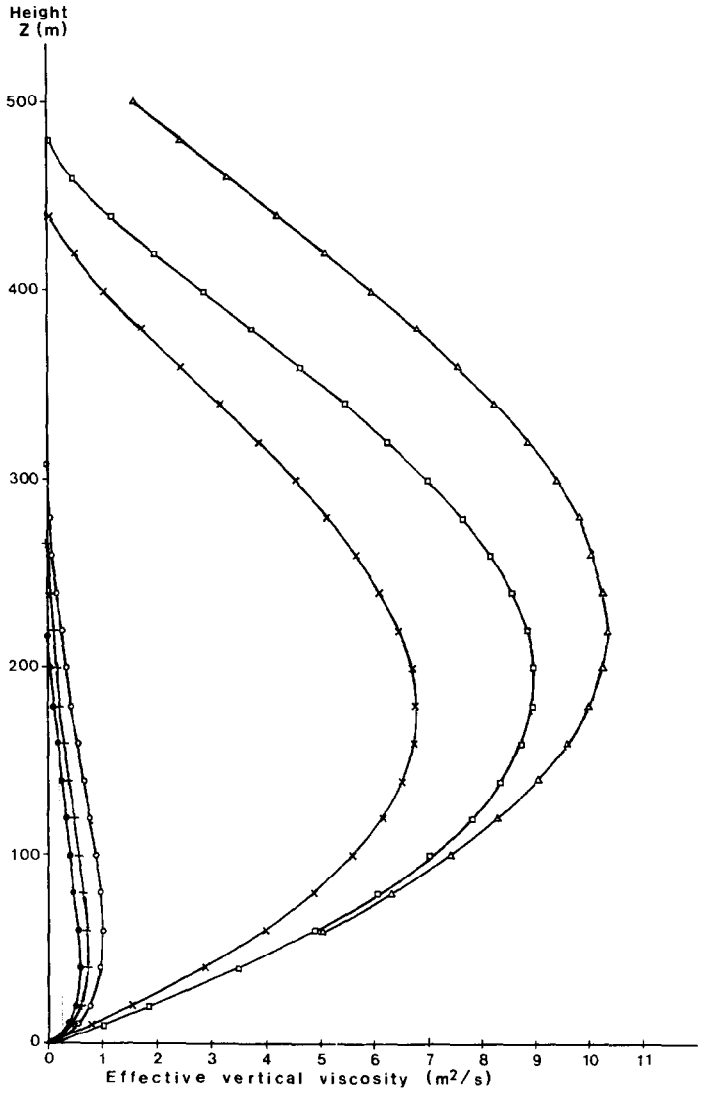

Fig. 7. Effective vertical viscosity. Conditions: —●— stable (2°C/100 m), + + stable (1°C/100 m), —○— stable (0°C/100 m), —×— neutral (−1°C/100 m), —□— instable (−2°C/100 m), and —△— instable (−4°C/100 m). $Z_0 = 0.03$ m, $v_{10\,m} = 3$ m/s.

4.3 Influence of atmospheric stability

The turbulence in the atmospheric boundary layer is described in a very detailed way based on the thermally and mechanically generated turbulence simulated by the vertical effective viscosity (see Fig. 7).

The atmospheric stability feature has been checked in comparing the BITC model with the Gaussian model under different Pasquill categories (neutral D, unstable A an stable F).There was close agreement between the BITC model and Gaussian predictions (see Fig. 5).

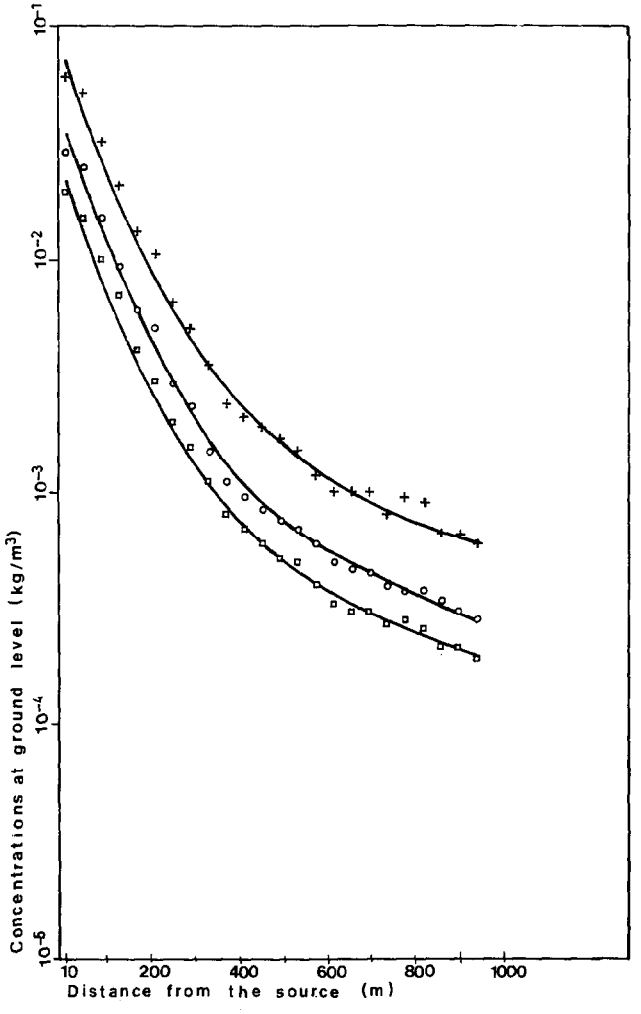

Fig. 8. Influence of the wind speed. Conditions: neutral atmosphere D, free field, continuous emission (10 kg/s) of chlorine, source at ground level, $Z_0 = 0.01$ m, $\nabla T = -1°C/100$ m. Wind speed at a height of 10 m ($v_{10\,m}$) in: + + 5 m/s, —○— 10 m/s, and —□— 15 m/s.

In Fig. 5 the wind speed is the same (3 m/s) for the three different stability categories chosen and the difference observed between the 3 dispersion curves is only due to the 3 different thermal gradients, ∇T, adopted ($-3°C/100$ m for unstable, $-1°C/100$ m for neutral and $+2°C/100$ m for stable).

4.4 Influence of the wind speed

To show the influence of the wind speed on dispersion, a 10 kg/s chlorine release in neutral atmospheric conditions has been assumed with 3 different

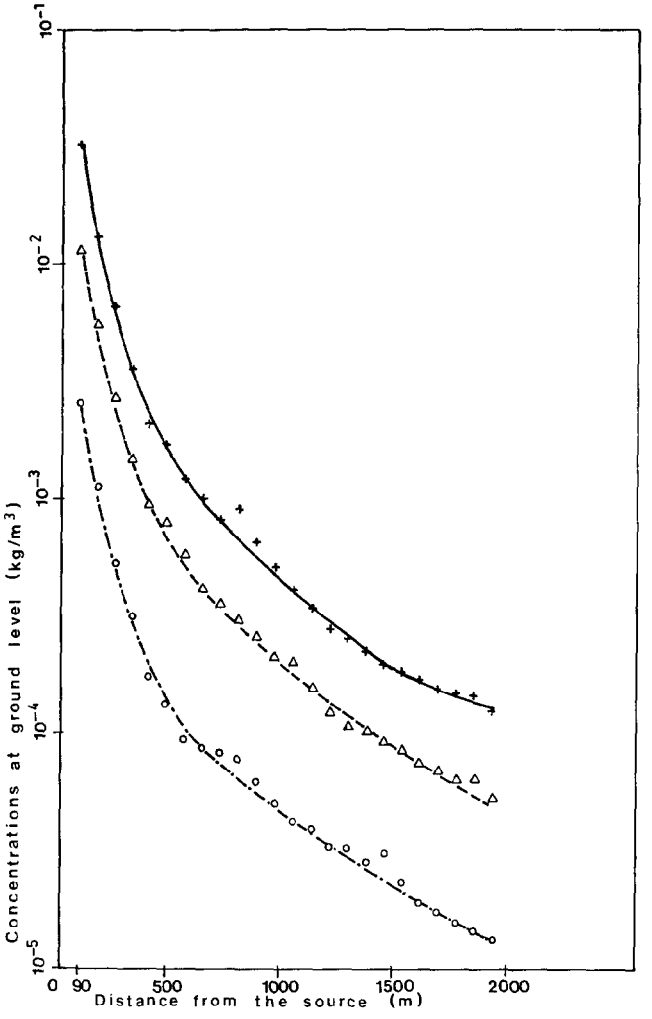

Fig. 9. Influence of the flowrate. Conditions: neutral atmosphere D, free field, continuous chlorine spill from a source at ground level, $Z_0 = 0.1$ m, $v_{10m} = 5$ m/s and $\nabla T = -1°C/100$ m. Release rate: + + 10 kg/s, − △ − 5 kg/s, and ·—○—· 1 kg/s.

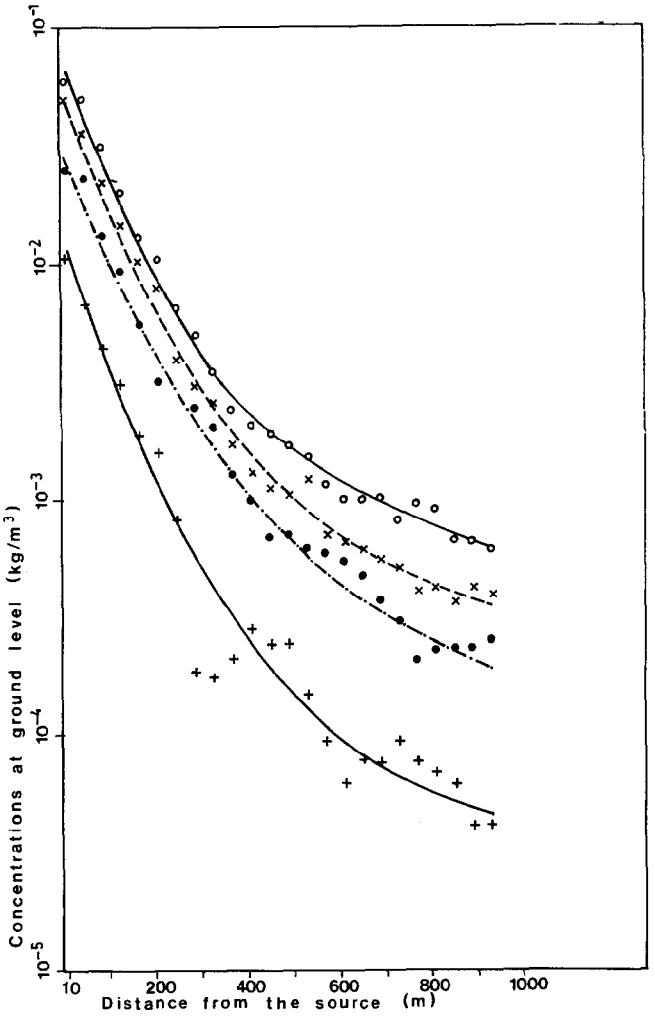

Fig. 10. Influence of the emission duration. Conditions: neutral atmosphere D, free field, continuous chlorine spill at 10 kg/s from a ground level source, $Z_0 = 0.1$ m, $v_{10m} = 5$ m/s, and $\nabla T = -1\,^{\circ}C/100$ m. Emission duration: —○— 1200 s, —×— 300 s, ·—●—· 60 s, and + + 10 s.

wind speeds (5, 10 and 15 m/s). As expected, dispersion is significantly improved as the wind speed increases (Fig. 8).

4.5 Influence of the pollutant release rate

The direct effect of the pollutant release rate on dispersion is clearly shown in Fig. 9 (isopleths), where a continuous emission of chlorine at ground level has been considered for 3 different release rates (1, 5 and 10 kg/s). As ex-

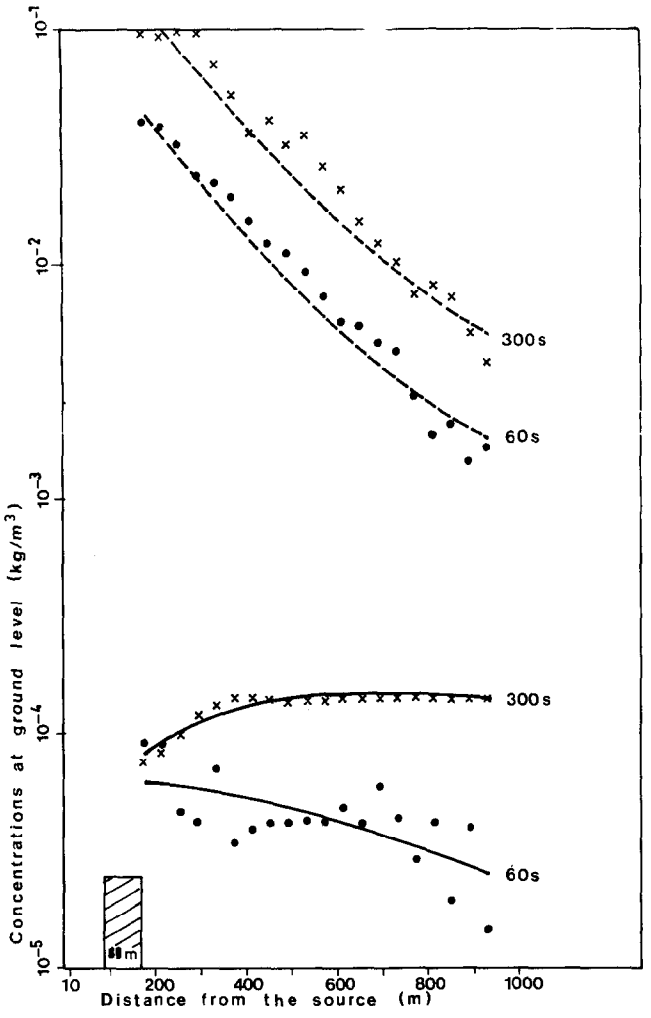

Fig. 11. Puffs of chlorine in stable atmosphere F. Conditions: source at groundlevel, flowrate 10 kg/s, $Z_0=0.1$ m, $v_{10\,m}=2$ m/s, building dimensions are $L=80$ m and $H=24$ m. $-\times-$ Free field (300 s), $\ast$ with building (300 s), $-\bullet-$ free field (60 s), and $-\bullet-$ with building (60 s).

pected, the ground level concentrations predicted depend linearly on the pollutant release rate.

4.6 Influence of the emission duration

To investigate the effect of the emission duration, a 10 kg/s release of chlorine at ground level in neutral atmospheric conditions has been assumed. Four different emission durations have been considered: 10, 60, 300 and 1200 s. Fig-

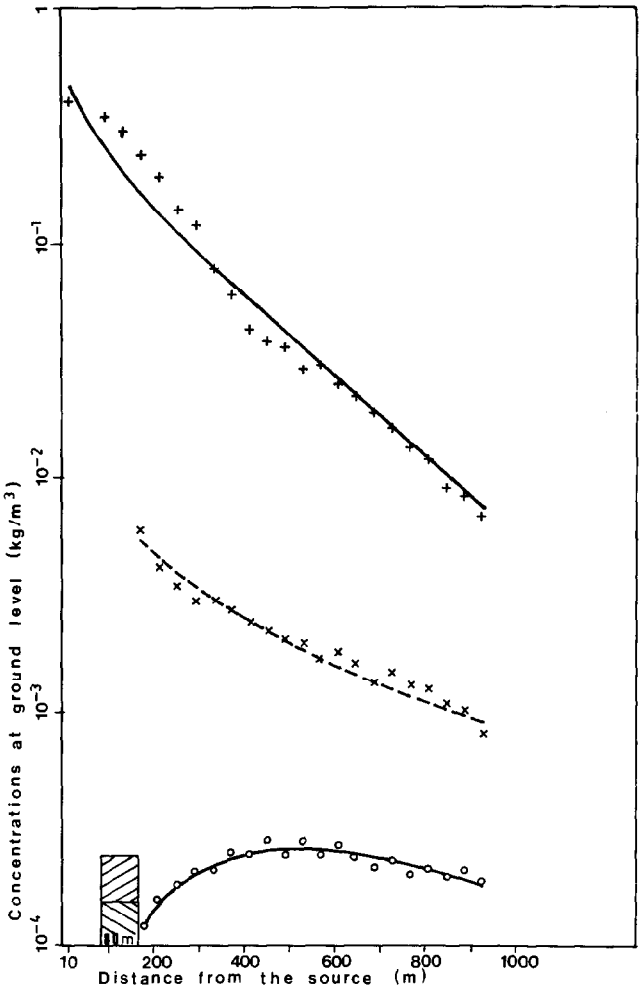

Fig. 12. Influence of buildings in stable atmosphere F. Conditions: continuous chlorine emission at 10 kg/s from a source at ground level, $Z_0=0.1$ m, $v_{10\,m}=2$ m/s, and $\nabla T=2°C/100$ m. + + Without building, −×− with building, ($H=12$ m), and −○− with building ($H=24$ m).

ure 10 shows the maximum ground level concentrations predicted by the BITC model in each case.

It appears that the effect of the emission duration is more important in the distant zone and less significant close to the source.

Moreover, it appears that in the neutral atmospheric conditions considered (with a wind speed of 5 m/s) the emission of 1200 s duration produces similar results to a continuous emission in the intermediate zone assumed (up to 1000 m from the source).

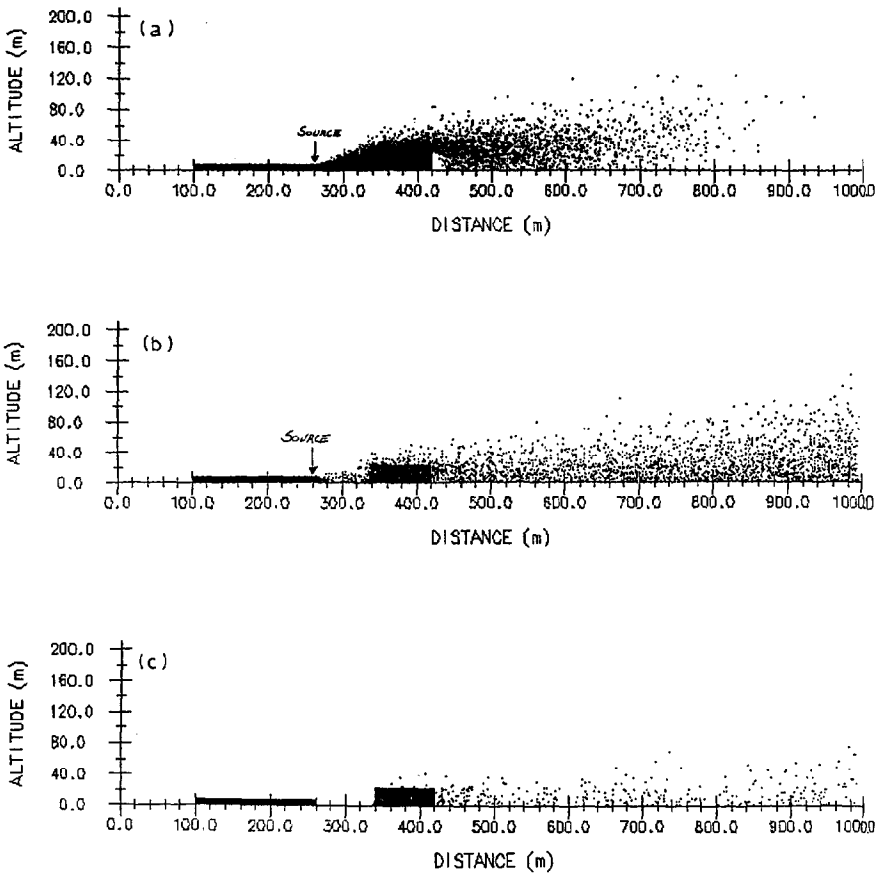

Fig. 13. Influence of buildings. Conditions see Fig. 12. (a) 240 s, (b) 600 s, and (c) 100 s ($H=24$ m).

4.7 Influence of 2-D buildings on dispersion

An important feature of the BITC model is its ability to take into account the effect of obstacles on the down-wind dispersion processes.

However, for the model's 2-D velocity field calculation to be valid, obstacles must be assumed to be infinite perpendicularly to the wind direction. This means that only a restricted selection of obstacles can be simulated, such as walls, large buildings, channels, roadways, and so on.

Figure 11 shows the effect of 2-D buildings interposed in the gas path. In the simulations performed, the buildings extend 80 m downwind and 2 different heights are considered (12 and 24 m). Because of the program limitation to two dimensions the buildings are assumed to extend laterally to infinity. The effect of buildings has been simulated for different atmospheric stability classes and different pollutant emission durations.

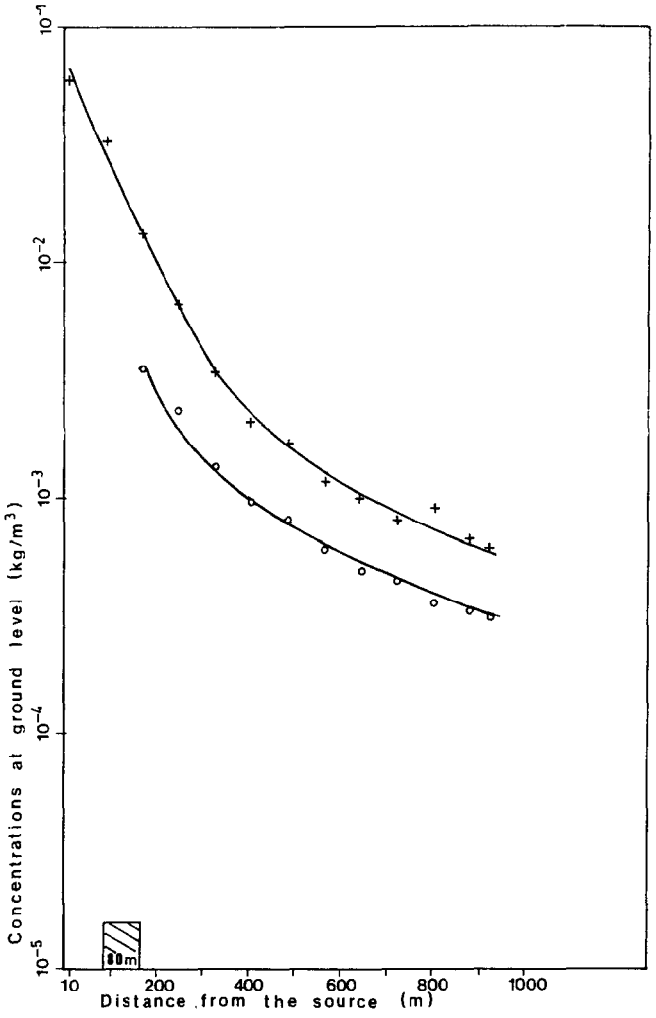

Fig. 14. Influence of a building in neutral atmosphere D. Continuous chlorine emission at 10 kg/s from a source at ground level, $Z_0=0.1$ m, $v_{10\,m}=5$ m/s, and $\nabla T=-1°C/100$ m. + + Without building, —O— with a 12 m high building, 80 m in the wind and 40 m in the cross wind direction.

It can be seen that the presence of obstacles in the gas path improves significantly the dispersion process, especially in stable atmosphere F (see Fig. 12).

Figure 13 shows the graphical distribution of the particles in the symmetry plane. Thanks to this useful pictorial representation, the behaviour of the particles in the vicinity of the obstacles is clearly shown.

4.8 Influence of finite 3-D obstacles

Although the model can in principle be used to solve the velocity field for a domain containing real 3-D obstacles, the required CPU time for the current generation of computers is impractically long.

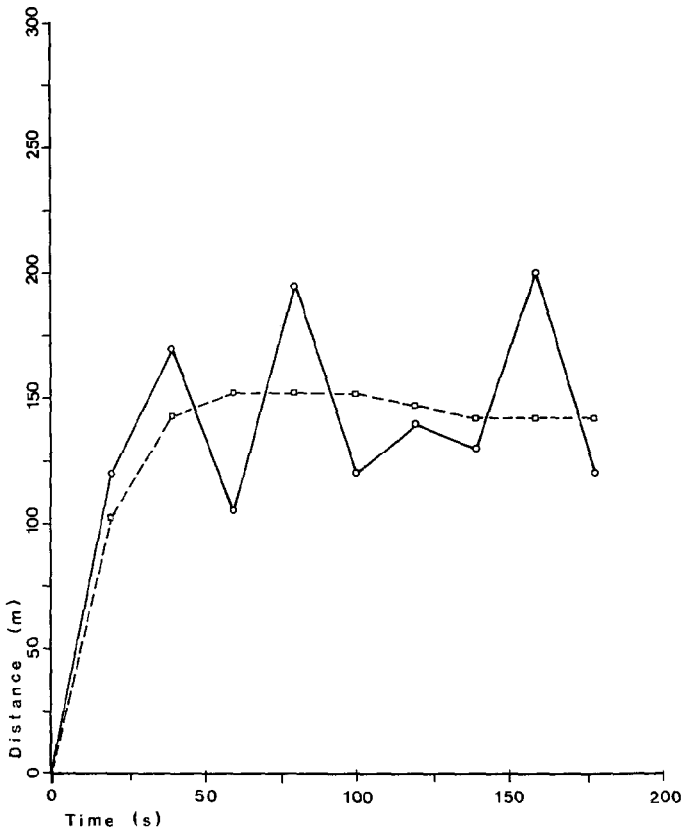

Fig. 15. BURRO 7: distance to the LEL. Conditions: 16.7 t LNG release at 347 t/h. —O— China Lake experiment, — □ — BITC simulation.

Consequently, the computer model has to be restricted to a 3-D field containing 2-D obstacles.

This restriction means that the gas is assumed to pass over the top of an obstacle in all cases, whereas in practice under some conditions, heavy gas would tend to bifurcate around an obstacle.

Thus, it was necessary to develop corrections to apply to the 2-D version of the BITC code to provide a practical method of modelling a field containing finite 3-D obstacles.

For this purpose, many experiments were performed in the wind tunnel at the Von Karman Institute. On the basis of these experiments it is possible to conclude that the critical parameter determining the behaviour of the gas plume is the width to height ratio of the obstacle.

In particular, the gas plume will tend to split and pass on either side of 3-D obstacles for plume width-to-height ratio smaller than or equal to 7. Empirical

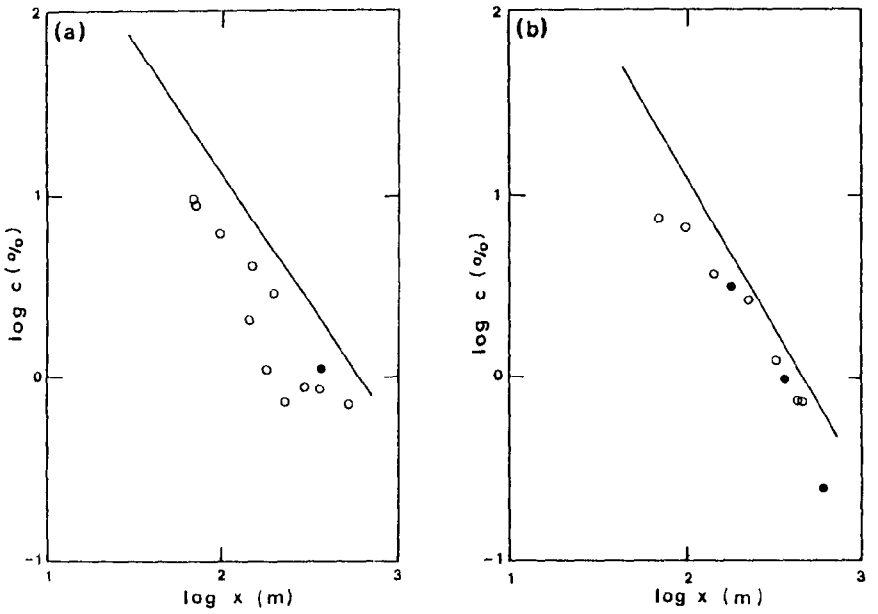

Fig. 16. Simulation of Thorney Island experiments. Solid lines are calculated at centerline, ○ measured at centerline, and ● measured near centerline. (a) Experiment 8, and (b) experiment. 13.

corrections have therefore been made to the 2-D programs to match wind-tunnel experimental data, and to enable practical dispersion behaviour to be modelled around a finite 3-D obstacle.

Figure 14 shows the ground-level concentrations predicted by the BITC programs when a finite 3-D obstacle is interposed in the chlorine gas path (width = 40 m, height = 12 m).

4.9 Comparison with the China Lake experimental releases

As explained previously, the BITC model was first validated against wind tunnel measurements and was then successfully checked against other models.

A complete validation of the BITC model also requires direct comparison with data obtained at full scale, whether by experiment or from well documented accidents. For this purpose, the results from the experimental releases of methane at China Lake in the BURRO tests were compared with simulations by the BITC program. Good agreement was found between the experimental results and the computed ones.

In Fig. 15 the distance to the LEL (Lower Explosive Limit) was plotted against time, both as measured experimentally and as calculated by the BITC program. The small difference between the curves is due to the fact that the

experimental results demonstrate the effect of random fluctuations in weather conditions which cannot be calculated predictively.

4.10 Comparison with Thorney Island experiment no. 13

This comparison was made by Schreurs [5]. Figure 16, reproduced from his work, shows the rather good agreement between calculated and observed values for Thorney Island experiments of heavy gas dispersion nos. 8 and 13.

5. Conclusions

The BITC computer code should now be considered as a valuable tool for investigating atmospheric dispersion of heavy gases in complex environments.

Its specificity makes it a complement to the existing less sophisticated models that are commonly used in industry when roughing out a problem.

The large test set that was set up in order to validate the code does represent a fairly significant set of industrial scenarios.

Taking into account the recent developments in computer science and hardware, we can expect reasonable computer times needed for an intensive use of the present code, on the one hand, and we are now able to emphasize both a 3-D version of the turbulent fluid flow and a refined description of what happens during the early stages of an accidental process, on the other.

Notation

A	constant in turbulence model
B	constant in turbulence model
C	constant in buoyancy production/loss term of turbulence model
c	concentration, kg/m^3
g	acceleration of gravity m/s^2
L	Monin–Obukhov length, m
L_d	length scale in turbulence model, m
Pr_t	turbulent Prandtl number
P_θ	production/loss term in turbulence model, m^2/s^2
Ri_g	gradient Richardson number
S	source term, kg/m^3
T	temperature, K
u	mean horizontal wind velocity, m/s
u_x	friction velocity, m/s
$v_{10\,m}$	windspeed at a height of 10 m, m/s
w	mean vertical velocity, m/s
x	downwind distance, m
y	cross-wind distance, m
z	height, m
Z_0	roughness height, m

Greek

μ_x	horizontal mechanical turbulent viscosity, m^2/s
μ_z	vertical mechanical turbulent viscosity, m^2/s
$\mu_{T,x}$	horizontal turbulent heat transfer coefficient, m^2/s
$\mu_{T,z}$	vertical turbulent heat transfer coefficient, m^2/s
θ_0	reference potential temperature, K
γ	kinematic viscosity of air m^2/s
ϕ	kinematic pressure (pressure divided by density), m^2/s^2
δ	boundary layer thickness, m
α	adjustable model parameter
∇	gradient

References

1 A. Foussat, Dispersion turbulente d'un polluant dans l'atmosphère, Thèse de Doctorat (Ph.D), Université Louvain-la-Neuve/Von Karman Institute, Brussels, 1980.

2 A. Foussat, Modèle de dispersion atmosphérique non-isotherme d'un polluant gazeux de densité quelconque en présence de non-uniformités orographiques, Von Karman Institute, Technical Note 135, January 1981.

3 J. van Diest, J.C. Basler, C. Benocci, D. Olivari, M.L. Riethmuller and E. Vergison, Atmospheric dispersion of heavy gases in a complex environment, C.E.C. contract no. ENV 713-B CRS, Final report, Brussels, 1986.

4 J.A. Businger, H. Tennekes, J.C. Wyngaard and S.J. Cauche, A short coarse on atmospheric turbulence and air pollution modelling, The Hague, D. Reidel Publ. Co. Dordrecht, 1981.

5 P. Schreurs, Mathematical modelling of the dispersion of accidental releases of heavy gases at ground level in an industrial environment, Ph.D. Thesis, Katholieke Universiteit Leuven, Leuven, 1983.

6 C. Benocci, D. Olivari and E. Vergison, Lagrangian modelling of turbulent dispersion layers, paper presented on 11th IMACS World Congress, Oslo, Norway, August 5-9, 1985.

7 P. Schreurs and J. Mewis, Development of a transport phenomena model for accidental releases of heavy gases in an industrial environment, Atmos. Environ., 21(4)(1987)765-776.

8 D.R. Blackmore, M.N. Herman and J.L. Woodward, Heavy gas dispersion models, J. Hazardous Mater., 6 (1982) 107-128.

9 E. Vergison, Travaux poursuivis dans le cadre du dévelopement des programmes de dispersion atmosphérique. Solvay Internal Report LC 3, 26 February 1982.

10 V.W. Nee and L.S.G. Kovasznay, Simple phenomenological theory of turbulent shear flows. Phys. Fluids, 12 (3) (1969) 473-484.

11 C.W. Hirt and J.L. Cook, Calculating 3-D flows around structure and over flat terrain J. Comp. Phys., 10 (1972) 32.

12 J.E. Welch, F.H. Harlow, J.P. Shannon and B.J. Daly, The Mac Method — A computer technique for solving viscous, incompressible, transient fluid-flow problems involving free surfaces. Los Alamos Laboratory, LA-3425, Los Alamos, NM, 1969.

13 A.A. Amsden and F.H. Harlow, The SMAC method: a numerical technique for calculating incompressible fluid-flows. Los Alamos Laboratory, LA-4370, Los Alamos, NM, 1970.

14 C. Benocci, D. Olivari and E. Vergison, Modelling of turbulent dispersion of neutral and buoyant contaminants released from 2-D sources, Von Karman Institute Technical Note 150, March 1984.
15 F. Pasquill, Atmospheric Diffusion, 2nd ed. Ellis Horwood, Chichester, 1974.
16 C. Benocci and D. Olivari, Development and improvement of the BITC dispersion model. Von Karman Institute for Fluid Dynamics, Brussels, CR. 1986, 10 April.
17 R.P. Koopman, R.T. Cederwall, D.L. Ermak, H.G. Goldware, Jr., W.J. Hogan, J.W. McClure, T.G. McRae, D.L. Morgan, H.C. Rodean and J.H. Shinn, Analysis of Burro series 40 m^3 LNG spill experiments, J. Hazardous Mater., 6 (1982) 43–83.
18 D.L. Ermak, S.T. Chan, D.L. Morgan and L.K. Mo, A comparison of dense gas dispersion model simulations with Burro series LNG spill text results, J. Hazardous Mater., 6 (1982) 129–160.
19 Risk Analysis of Six Potentially Hazardous Industrial Objects in the Rijnmond Area — A Pilot Study. D. Reidel, Dordrecht, 1982.
20 R.A. Cox and R.J. Carpenter, Further developments of a dense vapour cloud dispersion model for hazard analysis, in: Heavy Gas and Risk Assessment. D. Reidel, Dordrecht, 1980.
21 M.R. Beychok, Fundamentals of stack gas dispersion, 1979. M.R. Beychok, Irvine, CO.
22 Methoden voor het Berekenen van de Fysische Effekten van het Incidenteel Vrijkomen van Gevaarlijke Stoffen ('Yellow Book', in Dutch), 1979. Directoraat-Generaal van de Arbeid, Voorburg, The Netherlands.
23 A. Doury, Une méthode de calcul pratique et générale pour la prévision numérique des pollutions véhiculées par l'atmosphère. Rapport CEA-R-4280, 1972.
24 A.S. Monin and A.M. Obukhov, Basic laws of turbulent mixing in the atmosphere near the ground, Tr. Akad. Nauk. USSR Geofiz. Inst., 24 (151) (1954) 163–187.
25 M.L. Riethmuller and C. Borrego, Measurements and predictions of complex turbulent flows. Von Karman Institute LS 1980-03, Brussels.
26 D. Tordella, Influence of gravity forces on turbulence development. Von Karman Institute PR 1983-26, Brussels.
27 A.P. van Ulden, On the spreading of a heavy gas released near the ground, in: C.H. Bushmann (Ed.), Proc. 1st Int. Symp. on Loss Prevention and Safety Promotion in the Process Industries, Delft, The Netherlands. Elsevier, Amsterdam, 1974, pp. 221–226.
28 J. Havens, Personal communication, Brussels, 1988.